Research on the Prestress of Electromagnetic Launcher

Bo Gao(✉), Lie Tao, Xuguang He, Lizhou Wu, and Qunxian Qiu

Zhengzhou Institute of Mechanical and Electrical Engineering, Zhengzhou 450002, China
gaobo713@163.com

Abstract. The reasonable contact pressure between the armature and the rail is the core to ensure that no ablation occurs, and the application of a reasonable prestress to the launcher is an important way to ensure contact pressure. In this paper, using the finite element software ANSYS, the prestress application of typical railgun structure is compared and analyzed, and the traditional empirical formula is simulated and verified through tests, and the typical prestress application method of railgun is proposed. The research results of this paper have important guiding significance for the structural design of electromagnetic launcher.

Keywords: Railgun · Launcher · Contact pressure · Armature · Prestress

1 Introduction

Electromagnetic rail launch is a novel launch technique that uses electromagnetic forces to accelerate objects to hypervelocities [1–5]. Static analysis of railgun is an important means of the structural design of the railgun. In general, it is assumed that the Lorentz force acting on the rail is a uniformly distributed load on the inner surface of the rail [6]. Although the load applied to the rail is instantaneous, in order to ensure the contact stability between the armature and the rail during launching operation, it is usually necessary to apply a certain amount of prestress to control the deformation of the muzzle, ensure that appropriate contact pressure is maintained between the armature and the rail, and avoid the loss of contact between the armature and the rail due to excessive local temperature, which may cause armature vibration, transition arc and other phenomena [8–10].

Studies have shown that most contact transition phenomena are due to the loss of contact pressure [11]. Sufficient contact pressure can effectively increase the transition velocity during electromagnetic launch, while the contact pressure between the armature and the rail has a great influence on the launch process during the movement of the armature. During the operation of the electromagnetic railgun, the initial contact pressure is provided by the armature-rail mechanical pre-pressure. With the establishment of a magnetic field in the railgun bore, the electromagnetic force also provides some contact pressure. Excessive contact pressure may cause launch delay and surface wear, while on

K. Xie et al. (Eds.): ACCES 2022, LNEE 1014, pp. 1131–1139, 2023.
https://doi.org/10.1007/978-981-99-0408-2_120

the other hand, under the current shrinkage effect of the contact area, the contact area generates a separation force that promotes the armature to disengage from the rail, and insufficient contact pressure cannot overcome this force and thus lead to contact loss [11–16].

With reference to the above methods, this paper focuses on an empirical formula to simulate, compare and analyze the prestress of a typical railgun structure, and verify through small-scale test devices.

2 Calculation Model

2.1 Interface Model of Railgun Bore

Figure 1 is a schematic diagram of the cross-section of a typical railgun structure. It is mainlycomposed of rail, insulation support, inner encapsulation and outer encapsulation.

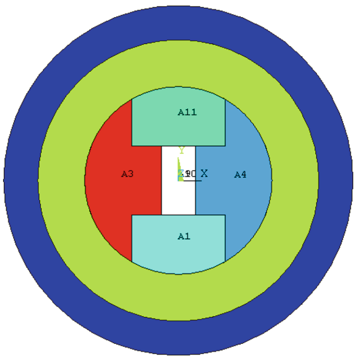

Fig. 1. The cross-section of the launcher

2.2 Rail Stress Analysis

Figure 2 shows the applied power curve. 1.1 MA current is applied at 0.5 to 2 ms and the current drops to 0 MA at 4 ms. The transient Lorentz force results from the interaction between the current flowing through the conductor and the resulting electromagnetic field. High transient load is the root cause of the armature and rail bearing forces.

For this structure, the force acting on the rail can be obtained by the relationship between two parallel conductors, and the calculation formula is as follows:

$$q = \frac{\mu I^2}{\pi b} \arctan\left(\frac{b}{2r}\right) \tag{1}$$

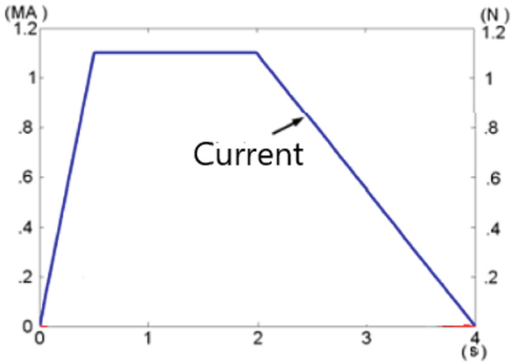

Fig. 2. The applied current waveform

where, μ indicates the vacuum permeability, b refers to the average width of the rail, and r represents the distance between the centers of the two rails. Therefore, the maximum distributed load acting on the rail is 4.22 MN/m, equivalent to a pressure load of 105.5 MPa. The list of railgun parameters is shown in Table 1 below:

Table 1. The main parameters of the launcher

S/N	Parameter name	Value
1	Rail length	2.75 m
2	Device caliber	30 × 15 mm
3	Projectile mass	600 g
4	Inductance gradient	0.461 uH/m

3 Comparative Analysis of Prestress

3.1 Analysis of Structure Without Prestress

Suppose the Lorentz force acting on the rail is a uniformly distributed load on the inner surface of the rail. Based on the axisymmetric characteristics of the structure, the 1/4 model is analyzed for plane problems. The model is shown in Fig. 3:

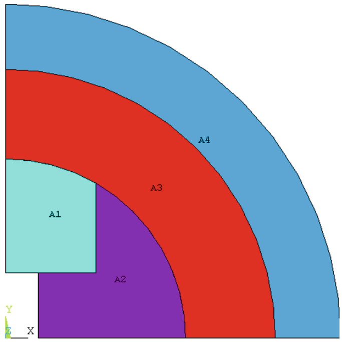

Fig. 3. The 1/4 simplified model of the launcher

In the calculation model, the rail is made of copper, the insulation support and the inner insulation encapsulation are made of epoxy phenolic glass cloth laminates, and the outer encapsulation is made of high-strength alloy steel. The list of mechanical properties of each material is shown in Table 2:

Table 2. The main material properties of the launcher

Material	Elastic modulus (Pa)	Poisson's ratio	Density (kg/ m3)	Elastic modulus (Pa)
Copper	127 E9	0.35	8900	127 E9
Epoxy phenolic	20 E9	0.16	1900	20 E9
Steel	207 E9	0.3	7800	207 E9

During the finite element analysis, the mesh is divided into 1414 elements. The materials are in contact with each other, and the contact element is surface-to-surface. A total of 4 contact pairs are defined, including the vertical contact pair between the rail and the insulation support, the contact pair between the inner insulation encapsulation and the rail, the contact pair between the inner insulation encapsulation and insulation support, and the contact pair between the outer encapsulation and the inner insulation encapsulation. Under the condition of no prestress, an expansion force load of 105.5 MPa is applied to the rail. The simulation results are shown in Fig. 4 and Fig. 5.

The simulation results of the launcher without prestress conditions demonstrate that:

1. Under the condition of no prestress, the rail bears a pressure load of 105.5 MPa, and the maximum equivalent stress generated is 206 MPa near the rail surface. The stress generated at the outer encapsulation is 140 MPa, and the stress generated at the insulation support and the inner insulation encapsulation is very small and can be ignored. A comparison of the strength limits of the above three materials shows that all three materials are within the safe range.

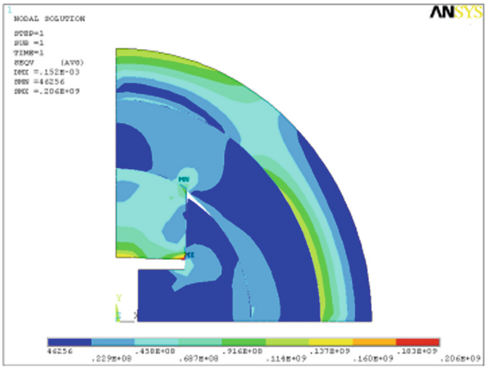

Fig. 4. The equivalent stress cloud map of the launcher without prestress conditions

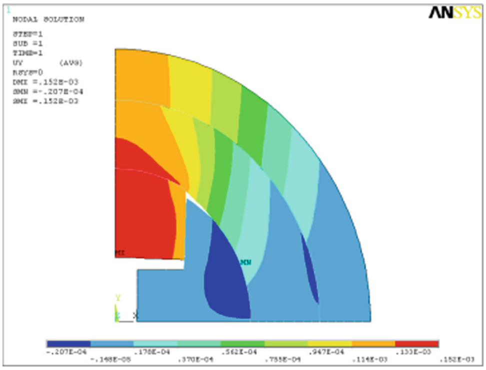

Fig. 5. The UY direction deformation of the launcher without prestress conditions

2. Under the condition of no prestress, the maximum strain in the UY direction occurs in the rail and the inner insulation encapsulation, and the unilateral strain in the UY direction of the overall structure is 0.152 mm. Therefore, the deformation of the railgun caliber can be obtained as follows:

$$\frac{0.152 \times 2}{30} \times 100\% = 1.013\% \tag{2}$$

3. According to the design experience of the railgun, in order to ensure good contact between the armature and the rail, it is generally required that the caliber deformation of the launcher is less than 1% during the projectile launch process. Therefore, under the condition of no prestress, although the stress borne by each structure of the railgun is within a safe range, the caliber deformation has exceeded the empirical value, and the dynamic launching may cause serious ablation, which does not meet the launching requirements.

3.2 Analysis of Structure with Prestress

Under the condition of constant expansion force load, prestress of 50 MPa is applied to the outer encapsulation surface according to the principle of "one gram force per ampere". Simulation results are shown in Fig. 6 and Fig. 7:

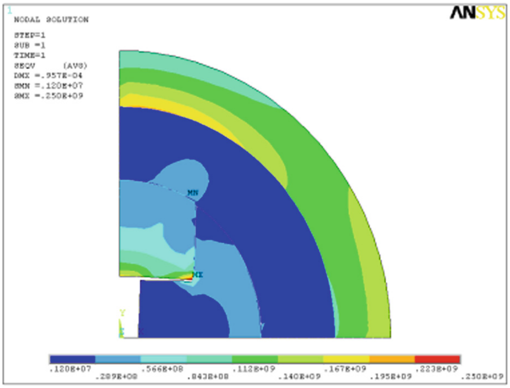

Fig. 6. The equivalent stress cloud map of the launcher with prestress conditions

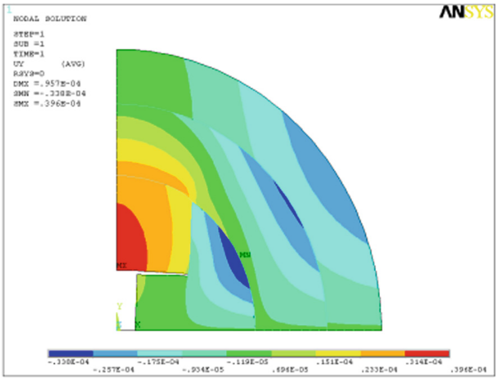

Fig. 7. The UY direction deformation of the launcher without prestress conditions

The simulation results of the launcher with prestress conditions demonstrate that:

1. When the rail is subjected to a pressure load of 105.5 MPa, the maximum equivalent stress generated under the condition of applying 50 MPa prestress as per the empirical formula of "one gram force per ampere" is 250 MPa, which occurs near the rail surface, and the stress generated at the outer encapsulation is 170 MPa. The stress generated at the insulation support and the inner insulation encapsulation is so small that can be ignored. By comparing the strength limits of the above three materials, it can be seen that the three materials are also within the safety range.

2. When the rail bears a pressure load of 105.5 MPa, the maximum strain in the UY direction occurs at the rail, and the unilateral strain in the UY direction of the overall structure is 0.0396 mm under the condition of applying 50 MPa prestress according to the empirical formula of “one gram force per ampere”. Therefore, the deformation of the railgun caliber can be obtained as:

$$\frac{0.0396 \times 2}{30} \times 100\% = 0.264\% \tag{3}$$

3. During the projectile launch with prestress conditions, the deformation of the launcher caliber is far less than 1%, which does not exceed the maximum caliber deformation range based on the empirical value, and the dynamic launching does not lead to ablation, which meets the launching requirements.

4 Test Verification

In order to further study the influence of prestress application on the launch state and verify the correctness of the empirical formula, a launch test without prestress (the deformation of railgun caliber is about 1.84%) and a test with prestress (the deformation of railgun caliber is about 0.92%) are carried out under the same armature and current conditions, respectively. After completion of the dynamic tests, the surface conditions of the rail are shown in Fig. 8 and Fig. 9:

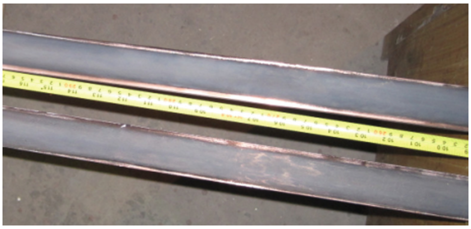

Fig. 8. The surface condition of the rail after the launcher testwithout prestress

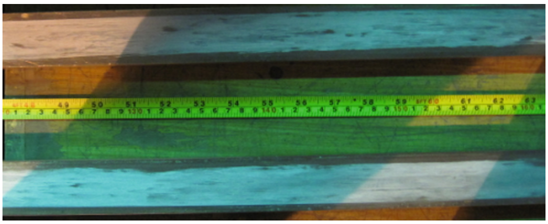

Fig. 9. The surface condition of the rail after the launcher test with prestress

Two dynamic launch tests show that application of prestress to the launcher according to the empirical formula of "one gram force per ampere" can fully keep bore deformation within 1%, thus avoiding poor contact between the armature and the rail during launching. This principle is also one of the important means to realize launch without ablation.

5 Discussion on Prestress Application Method

The above analysis shows that in the structural design process of railgun, in order to reduce muzzle deformation, it is very necessary to apply a certain amount of prestress. Throughout the development history of railgun and the current research progress at home and abroad, bolt pre-tightening, hydraulic pre-tightening or circular encapsulation structure for pre-tightening are mostly used in the laboratory, but the above methods have prominent disadvantages such as heavy structure. However, with the continuous development of engineering prototypes, carbon fiber winding for pre-tightening force has gradually become a mainstream pre-tightening scheme, and is widely used by domestic and foreign research teams. The empirical formula described in this paper is also suitable for the design of carbon fiber winding launchers.

6 Conclusions

1. In the structural design process of railgun, the influence of prestress on the deformation of the railgun cross-section must be considered. Generally, the deformation of railgun caliber should be controlled within 1% during launching.
2. Although there are many ways to apply prestress, the appropriate application method should be choosed according to the design purpose.
3. The "one gram force per ampere" empirical formula can be used to guide the design of the launcher as a principle of prestress application.

References

1. Yang, F.: Study on Transient Temperature Effect of Rail Inelectromagnetic Launch. Tianjin University, Tianjin (2020). (in Chinese)
2. McNab, I.R., Crawford, M., Satapathy, S., et al.: IAT armature development. IEEE Trans. Plasma Sci. **39**(1), 442–451 (2011)
3. Satapathy, S., Vanicek, H.: Down-slope contact transitionin railguns. IEEE Trans. Magn. **43**(1), 402–407 (2007)
4. Chen, W.H., Zhou, M.L., Yan, X.H., Li, Z.X., Lin. X.X.: Study on electromagnetic-fluid-temperature multiphysics field coupling model for drum of mine cable winding truck. China Electrotech. Soc. Trans. Electr. Mach. Syst. **5**(2), 133–142, 2021
5. Hsieh, K.T., Satapathy, S., Hsieh, M.T.: Effects of pressure-dependent contact resistivity on contact interfacial conditions. IEEE Trans. Magn. **45**(1), 313–318 (2009). (in Chinese)
6. Sikhanda, S., Harold, V.: Down-slope contact transition in railguns. IEEE Trans. Magn. **43**(1), 402–407 (2007)

7. James, T., James, D.: Contact pressure distribution and transition in solid armatures. IEEE Trans. Magn. **37**(1), 81–85 (2001)
8. Sikhanda, S., Trevor, W., Chadee, P.: Effect of geometry change on arma-ture behavior. IEEE Trans. Magn. **43**(1), 408–412 (2007)
9. Laura, R., Sikhanda, S., Kuo-Ta, H.: Effect of geometry change on the current density distribution in C-shaped armatures. IEEE Trans. Magn. **39**(1), 72–75 (2003)
10. Hsieh, K.T., Satapathy, S., Hsieh, M.T.: Effects of pressure-dependent contact resistivity contact interfacial conditions. IEEE Trans. Magn. **45**(1), 313–318 (2009)
11. Zhou, L., Lu, T.C., Zhang, B., et al.: Multi-physics coupling analysis of rough surfaces using 3D fractal model. Trans. China Electrotech. Soc. **30**(14), 226–232 (2015). (in Chinese)
12. Chen, Z.H., Tang, B., Shi, G., et al.: Optimal pressure load under multi-objective sliding electric contact in the pantograph-catenary system. Trans. China Electrotech. Soc. **30**(17), 154–160 (2015). (in Chinese)
13. Jin, L.W., Li, J.: Similarity of lubrication in armature-rail interface under the condition of electromagnetic railgun's physical field scaling method. High Volt. Eng. **42**(9), 2850–2856 (2016). (in Chinese)
14. Li, B., Lu, J.Y., et al.: Effect of interfacial roughness of sliding electrical contact on the melting characteristics of armature. Trans. China Electrotech. Soc. **33**(7), 1607–1615 (2018). (in Chinese)
15. Du, C.T., Lei, B., et al.: Research progress on armature technology in electromagnetic railgun. J. Gun Launch Control **38**(2), 94–100 (2017). (in Chinese)
16. Geng, Y.Q., Liu, H., et al.: Armature and rail's dynamic joule heating characteristic of the electromagnetic railguns. High Volt. Eng. **45**(3), 799–804 (2019). (in Chinese)